



# CHORUS

This is the accepted manuscript made available via CHORUS. The article has been published as:

## Heisenberg-Limited Qubit Read-Out with Two-Mode Squeezed Light

Nicolas Didier, Archana Kamal, William D. Oliver, Alexandre Blais, and Aashish A. Clerk  
Phys. Rev. Lett. **115**, 093604 — Published 27 August 2015

DOI: [10.1103/PhysRevLett.115.093604](https://doi.org/10.1103/PhysRevLett.115.093604)

# Heisenberg-limited qubit readout with two-mode squeezed light

Nicolas Didier,<sup>1,2</sup> Archana Kamal,<sup>3</sup> William D. Oliver,<sup>3,4</sup> Alexandre Blais,<sup>2,5</sup> and Aashish A. Clerk<sup>1</sup>

<sup>1</sup>*Department of Physics, McGill University, 3600 rue University, Montreal, Quebec H3A 2T8, Canada*

<sup>2</sup>*Département de Physique, Université de Sherbrooke, 2500 boulevard de l'Université, Sherbrooke, Québec J1K 2R1, Canada*

<sup>3</sup>*Research Laboratory of Electronics, Massachusetts Institute of Technology, Cambridge, MA 02139, USA*

<sup>4</sup>*MIT Lincoln Laboratory, 244 Wood Street, Lexington, MA 02420, USA*

<sup>5</sup>*Canadian Institute for Advanced Research, Toronto, Canada*

We show how to use two-mode squeezed light to exponentially enhance cavity-based dispersive qubit measurement. Our scheme enables true Heisenberg-limited scaling of the measurement, and crucially, is not restricted to small dispersive couplings or unrealistically long measurement times. It involves coupling a qubit dispersively to two cavities, and making use of a symmetry in the dynamics of joint cavity quadratures (a so-called quantum-mechanics-free subsystem, QMFS). We discuss the basic scaling of the scheme and its robustness against imperfections, as well as a realistic implementation in circuit quantum electrodynamics.

PACS numbers: 42.50.Dv, 03.65.Ta, 42.50.Lc, 03.67.-a, 42.50.Pq

*Introduction*— Research in quantum metrology has established that squeezed light and entanglement are key resources needed to approach truly fundamental quantum bounds on measurement sensitivity [1]. Perhaps the best known application is interferometry: by injecting squeezed light into the dark port of an interferometer, one dramatically enhances its sensitivity to small phase shifts [2, 3], reducing the imprecision below the shot-noise limit. Many of these ideas for squeezing-enhanced measurement were first motivated by gravitational wave detection [4–6], and have recently been implemented in current-generation detectors [7, 8]. More generally, squeezed light has been used to enhance the measurement sensitivity in optomechanics [9] and even biology [10].

Ultra-sensitive detection is also essential for quantum information processing where fast, high-fidelity qubit readout is required to achieve fault-tolerant quantum computation [11]. A ubiquitous yet powerful approach is dispersive readout, where a qubit couples to a cavity such that the cavity frequency depends on the qubit state, see e.g. [12]. The readout consists of driving the initially empty cavity with a coherent tone, resulting in a qubit-state dependent cavity field which is displaced in phase space from the origin [see Fig. 1(a)]. High-fidelity readout can then be obtained by measuring the output field quadratures. This is the standard approach used in state-of-the-art experiments with superconducting qubits, e.g. [13–15].

As with interferometry, one might expect that dispersive qubit measurement could be enhanced by using squeezed light. The most obvious approach would be to squeeze the phase quadrature of the incident light [i.e.  $Y$  in Fig. 1(b)], thus reducing the overlap between the two pointer states. As discussed recently in Ref. 16 the situation is not so simple, as the dispersive interaction will lead to a qubit-dependent rotation of the squeezing axis. Unlike standard interferometry, this rotation is a prob-

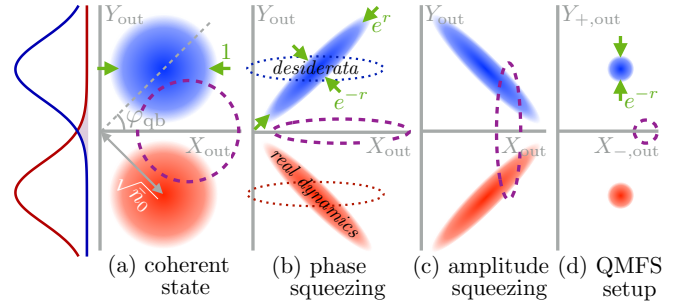


FIG. 1. Phase-space representation of dispersive qubit readout for different input states: (a) coherent state, (b) single-mode phase-squeezed state, (c) amplitude-squeezed state, (d) two-mode squeezed state in the QMFS ( $X_-$ ,  $Y_+$ ). The purple dashed lines represent the input state and the blobs represent the output fields. The input state is displaced along the  $X$ -axis and the signal is encoded in the quadrature corresponding to the  $Y$ -axis with homodyne detection; as depicted in the leftmost panel, the readout error corresponds to the overlap of the two marginals. Dispersive interaction with the qubit rotates the output field by the angle  $\varphi_{qb}$  for the ground state  $|0\rangle$  (in blue) and  $-\varphi_{qb}$  for the excited state  $|1\rangle$  (in red). Ideally, one wants the output state to be phase squeezed regardless of qubit state [dotted “desiderata” states in (b)]; this is not possible when using single-mode squeezing due to the qubit-induced rotation. Our new QMFS scheme [panel (d)] does not suffer from this problem.

lem, as optimal dispersive qubit readout involves large couplings and hence large rotations. Further complexity arises from the fact that this rotation is frequency-dependent. The upshot is that measurement always sees the amplified noise associated with the anti-squeezed quadrature of the incident light, limiting the fidelity improvement from using squeezing to modest values and preventing true Heisenberg-scaling [16].

Despite the above difficulties, we show in this Letter that it is indeed possible to substantially improve dis-

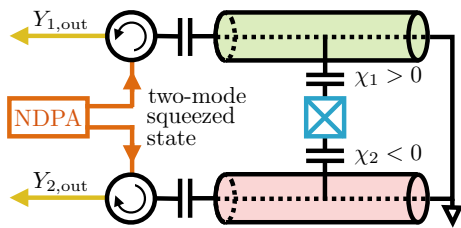


FIG. 2. Circuit QED implementation of QMFS dispersive qubit readout with two-mode-squeezed states produced by a non-degenerate paramp (NDPA). The signal is encoded in the joint quadrature  $Y_{+,out} \propto Y_{1,out} + Y_{2,out}$ ; see text for details.

persive qubit measurements using squeezed input states. Our proposed scheme involves using two-mode squeezed states in a two-cavity-plus-qubit system (see Fig. 2), which can lead to exponential enhancement of the signal-to-noise ratio (SNR) in dispersive measurement and achieves true Heisenberg-limited scaling. This is possible even for large qubit-induced phase shifts, and is thus in stark contrast from previous schemes using two-mode squeezing for interferometry [3] or qubit readout [16].

The key to our scheme is the use of a special dynamical symmetry, whereby two commuting collective quadratures exhibit a simple rotation as a function of time. As these quadratures commute, they constitute a so-called “quantum-mechanics-free subsystem” (QMFS) [17] and can both be simultaneously squeezed. The upshot is that one can effectively make a dispersive qubit measurement where now the uncertainties associated with the two pointer states are not limited by the uncertainty principle [see Fig. 1(d)]. Though the scheme is extremely general, for concreteness we explicitly discuss an implementation in circuit quantum electrodynamics (QED) using a transmon qubit [18], as depicted in Fig. 2.

The dynamical symmetry used in our two-mode scheme crucially relies on one of the cavities having an effective negative frequency; it is thus related to an idea first discussed in the context of measurement by Tsang and Caves [19] and Wasilewski et al. [20], and which has since been applied to other systems [17, 21, 22]. While many applications use the idea to suppress the effects of backaction [20–22], we instead use it as an effective means to exploit squeezed input light. Unlike previous studies, we calculate here the scaling of the resulting measurement sensitivity, showing that one obtains Heisenberg-limited scaling with incident photon number.

*Dispersive measurement and standard squeezing*– We start by reviewing the simplest setup where a qubit dispersively couples to a single-sided cavity (frequency  $\omega_1$ ) with the Hamiltonian  $H = (\omega_1 + \chi\hat{\sigma}_z)\hat{a}^\dagger\hat{a}$  [12]. Standard dispersive readout involves driving the input port of the cavity with a coherent tone at the cavity frequency (photon flux  $\bar{n}_0\kappa/4$ ,  $\kappa$  is the cavity damping rate). As illustrated in Fig. 1(a), as a consequence of the disper-

sive coupling, the output field is rotated by the angle  $\varphi_{qb} = 2 \arctan(2\chi/\kappa)$  if the qubit is in the ground state  $|0\rangle$  and by  $-\varphi_{qb}$  for the excited state  $|1\rangle$ . Writing the output field as  $\hat{a}_{out}(t) = e^{-i\omega_1 t}(\hat{X}_{out} + i\hat{Y}_{out})/2$ , for a displacement along the real axis  $X_{out}$ , the signal of the qubit state is encoded in the phase quadrature  $Y_{out}$ ; this quadrature is then recorded with homodyne detection.

Measuring  $Y_{out}$  for an integration time  $\tau$  corresponds to evaluating the dimensionless measurement operator  $\hat{M} = \sqrt{\kappa} \int_0^\tau dt \hat{Y}_{out}(t)$ . The signal is the qubit-state dependent expectation value  $M_S = \langle \hat{M} \rangle$  and is the same for all the injected states depicted in Fig. 1. The imprecision noise is the variance of the noise operator  $\hat{M}_N = \hat{M} - M_S$ . The signal-to-noise ratio  $\text{SNR} \equiv |M_{S,|0\rangle} - M_{S,|1\rangle}| / (\langle \hat{M}_{N,|0\rangle}^2 \rangle + \langle \hat{M}_{N,|1\rangle}^2 \rangle)^{1/2}$  is, for this coherent state dispersive readout,  $\text{SNR}_\alpha(\tau) \simeq |\sin \varphi_{qb}| \sqrt{2\bar{n}_0\kappa\tau}$  [23, 24]. As expected, the SNR is maximized for a phase  $\varphi_{qb} = \pi/2$ ; it also scales as  $\sqrt{\bar{n}_0}$ , akin to standard quantum-limit scaling in interferometry [1].

Next, consider what happens if we instead inject a displaced squeezed state (squeeze parameter  $r$ ) into the cavity. As already discussed, this is not as beneficial as one would hope, as one always sees the noise of the anti-squeezed quadrature ( $\propto e^{2r}$ ) [16, 25]. Consider the optimal case  $\varphi_{qb} = \pi/2$  which maximizes the signal. For large  $\tau$ , the noise behaves as

$$\langle \hat{M}_N^2 \rangle \simeq \kappa\tau [\sin^2(\theta)e^{-2r} + \cos^2(\theta)e^{2r}] + 2\sqrt{2} \sinh(2r) \cos(2\theta - 3\pi/4), \quad (1)$$

where we have dropped terms that decay exponentially with  $\kappa\tau$ . The first line of Eq. (1) dominates in the long-time limit, and represents the contribution from zero-frequency noise in the output field. For this line, the choice  $\theta = \pi/2$  cancels the contribution from the amplified quadrature, and leads to an exponential reduction in the noise compared to a coherent state drive [16]. In contrast, the second line of Eq. (1) describes the contribution from initial short-time fluctuations; the noise from the anti-squeezed quadrature here remains even if  $\theta = \pi/2$ . As a result, increasing  $r$  indefinitely does not improve the SNR; for a given  $\tau$  there is an optimal value [see Fig. 3 (b–c)]. This then leads to generally modest enhancement of SNR compared to a simple coherent state drive [16]; in particular, there is almost no improvement in the most relevant case where  $\tau \sim 1/\kappa$  [shaded region in Fig. 3(a)]. Optimized squeezing leads at best to the scaling  $N^{3/4}$  with input photon number, similar to a Mach-Zehnder interferometer driven with squeezed light [1, 2, 25].

*Negative-frequencies and two-mode squeezing*– To avoid having the measurement corrupted by the anti-squeezed quadrature, one ideally wants to squeeze *both* quadratures of the input light. While this is impossible with a single cavity, it becomes conceivable using joint quadratures of two cavities. If  $\hat{a}_j = (\hat{X}_j + i\hat{Y}_j)/2$  ( $j = 1, 2$ )

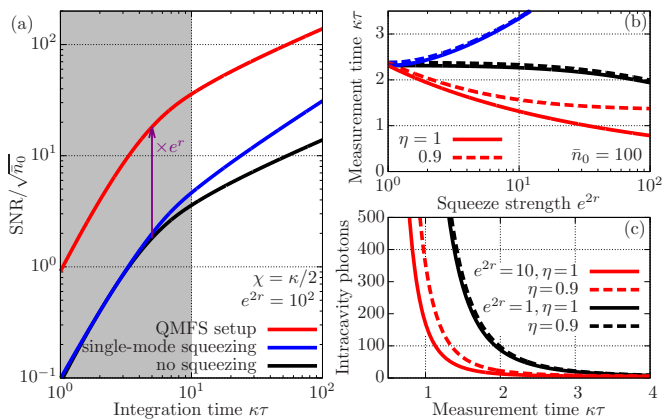


FIG. 3. (a) SNR as a function of integration time  $\tau$  for different protocols: coherent state drive (black), displaced single-mode squeeze state (blue), two-mode squeezed QMFS setup (red). We assume an optimal dispersive shift  $\chi = \kappa/2$ ; for the QMFS setup the cavity is pre-squeezed ( $t_0 \ll -1/\kappa$ ) with squeeze strength  $e^{2r} = 100$ . The coherent drive is turned on at  $\tau = 0$ . For the single-mode case, for each  $\tau$  we optimize the squeeze strength  $e^{2r} \in [1, 100]$  and angle (see [25]). The QMFS scheme gives an exponential SNR enhancement, especially in the most interesting regime where  $\tau \sim 1/\kappa$  (shaded region). (b) Integration time  $\tau$  required to achieve a fidelity  $F = 99.99\%$ , as a function of  $e^{2r}$ ; parameters as in (a), except that  $\bar{n}_0 = 100$ . Black lines correspond to an unsqueezed drive, where the drive strength is increased such that the intracavity photon number is the same as in the QMFS scheme, i.e.  $\bar{n}_0 \rightarrow \bar{n}_0 + 4 \sinh^2 r$ . The solid curves correspond to the case of no photon losses (efficiency  $\eta = 1$ ), while the dashed curves correspond to  $\eta = 0.9$ . (c) Total intracavity photon number needed to achieve  $F = 99.99\%$  in a measurement time  $\tau$ . Even with non-zero photon losses, the use of squeezing can dramatically reduce the number of intracavity photons.

are the annihilation operators for the two cavities (in an interaction picture with respect to the free cavity Hamiltonians), we define  $\hat{X}_\pm = (\hat{X}_1 \pm \hat{X}_2)/\sqrt{2}$ ,  $\hat{Y}_\pm = (\hat{Y}_1 \pm \hat{Y}_2)/\sqrt{2}$ . Since  $X_-$  and  $Y_+$  commute, they can be squeezed simultaneously, resulting in a two-mode-squeezed state [26]. The relevant non-zero input-field noise correlators are  $\langle \hat{X}_\mp(t) \hat{X}_\mp(t') \rangle = \langle \hat{Y}_\pm(t) \hat{Y}_\pm(t') \rangle = e^{\mp 2r} \delta(t - t')$ . We stress that such states have already been produced in circuit QED [27, 28].

This squeezing by itself is not enough: we also need the dynamics of these joint quadratures to mimic the behaviour of  $\hat{X}$  and  $\hat{Y}$  in a single cavity, such that the two qubit states still give rise to a simple rotation of the vector formed by  $(X_-, Y_+)$ . Such a dynamics is generated by the simple Hamiltonian [19, 20]

$$H = \frac{1}{2} \chi (\hat{X}_+ \hat{X}_- + \hat{Y}_+ \hat{Y}_-) \hat{\sigma}_z = \chi (\hat{a}_1^\dagger \hat{a}_1 - \hat{a}_2^\dagger \hat{a}_2) \hat{\sigma}_z. \quad (2)$$

The qubit thus needs to couple dispersively to both cavities, with equal-magnitude but opposite-signed couplings. The resulting dynamics is illustrated in Fig. 1(d): an incident field with  $\langle \hat{Y}_+ \rangle = 0$ ,  $\langle \hat{X}_- \rangle \neq 0$  is rotated in a qubit-state dependent manner, resulting in an output

field with  $\langle \hat{Y}_+ \rangle \neq 0$  (i.e. the measurement signal). Note that the squeezed quadratures  $X_-, Y_+$  are never mixed with the anti-squeezed quadratures  $X_+, Y_-$ , hence this amplification will not limit our scheme. We also stress that the two cavities need not have the same frequency.

The measurement protocol involves first turning on the vacuum two-mode squeezed drive at a time  $t = t_0 \leq 0$ , and then turning on the coherent cavity drive(s) at  $t = 0$ . This coherent drive (which displaces along  $X_-$  but not  $Y_+$ ) could be realized by driving one or both the cavities. We take the optimal case where both cavities are driven and let  $\bar{n}_0 \kappa / 8$  denote the photon flux incident on each cavity due to the coherent drives. The measurement signal in  $Y_+$  can be constructed from the quadratures  $Y_{j,\text{out}}$  of the output field leaving each cavity. In what follows, we consider the limit  $\kappa t_0 \ll -1$ , such that the measurement is not corrupted by any initial non-squeezed vacuum in the cavity [25].

The measurement operator is now  $\hat{M} = \sqrt{\kappa} \int_0^\tau dt \hat{Y}_{+, \text{out}}(t)$ . As expected, one finds that this output quadrature is always squeezed, and hence the imprecision noise is always described by  $\langle \hat{M}_N^2 \rangle = e^{-2r} \kappa \tau$ , independent of  $\chi$ . As desired, the noise is now exponentially reduced with respect to standard dispersive readout, leading to an exponential improvement of SNR, i.e.  $\text{SNR}_r(\tau) = e^r \text{SNR}_\alpha(\tau)$  for all integration times  $\tau$ . This is in stark contrast to the single-mode approach, where such an enhancement was only possible at extremely long times,  $\kappa \tau \gtrsim e^{4r}$  [c.f. Eq. (1)]. The SNR is plotted in Fig. 3(a) as a function of integration time  $\tau$ , with comparisons against the single-mode squeezing and no-squeezing cases; our two-mode scheme realizes dramatic improvements in the most interesting regime where  $\tau$  is not much larger than  $1/\kappa$ . The integration time  $\tau$  required to achieve a measurement fidelity  $F = 1 - \text{erfc}(\text{SNR}/2)/2$  of 99.99% is plotted against squeezing strength in Fig. 3(b). Again, the QMFS scheme results in dramatic improvements.

*Heisenberg-limited scaling*— We now show that the SNR scales as the number of photons  $N$  used for the measurement rather than its square root  $\sqrt{N}$  as it is the case for the standard dispersive readout [1]. For this, we define the temporal mode  $\hat{A} = \frac{1}{\sqrt{\tau}} \int_0^\tau dt [\hat{d}_{\text{in},1}(t) + \hat{d}_{\text{in},2}(t)]$  [3] where the operator  $\hat{d}_{\text{in},j}$  describes fluctuations in the resonator- $j$  input field. The total number of input photons  $N = N_s + N_d$  has a contribution from squeezing  $N_s = \langle \hat{A}^\dagger \hat{A} \rangle = 2 \sinh^2 r$  and  $N_d$  from the coherent displacement. Focusing on times  $\tau \gg 1/\kappa$ , we can ignore the transient response to the coherent drive, and hence  $N_d = \frac{1}{4} \bar{n}_0 \kappa \tau$ . Fixing  $N$  and taking  $t_0 \ll -1/\kappa$ , the optimal SNR is obtained for  $N_s = N^2 / [2(N + 1)]$ , and is

$$\text{SNR}_{\text{opt}} = 2 |\sin \varphi_{\text{qb}}| N \sqrt{1 + 2/N} \rightarrow 2 |\sin \varphi_{\text{qb}}| N, \quad (3)$$

where we have taken the large  $N$  limit. Eq. (3) corresponds to true Heisenberg scaling for any value of the

dispersive coupling. Such scaling is *not* possible using single-mode squeezed input light (see [25]).

Our QMFS scheme also shows an improved, Heisenberg-like scaling of the SNR with the intracavity photon number  $\bar{n}$ . Note that the SNR for the QMFS scheme has the same form as the SNR for a standard ( $r = 0$ ) dispersive readout made using a larger drive flux  $\bar{n}_0 e^{2r}$ . If we fix the intracavity photon number  $\bar{n} = \bar{n}_0 \cos^2(\varphi_{\text{qb}}/2) + 2 \sinh^2 r$  and optimize  $r$ , the resulting SNR scales as  $\text{SNR}_{\text{opt}} \simeq 2 |\sin(\varphi_{\text{qb}}/2)| \bar{n} \sqrt{\kappa \tau}$ , as opposed to the conventional  $\text{SNR}_\alpha \propto \sqrt{\bar{n}}$ .

*Robustness against imperfections*— Our discussion of the QMFS scheme so far has assumed a broadband, pure squeezing source. The purity of the squeezing is, however, not crucial; our scheme is insensitive to the anti-squeezed quadratures, and hence it is not essential that their variances be as small as possible. For a finite squeezing bandwidth  $\Gamma$ , the input squeezing spectrum will typically have a Lorentzian lineshape [29]. We find that the effects of a finite bandwidth are equivalent to an effective reduction of the squeezing strength; the SNR for the scheme is simply reduced by a prefactor  $\sqrt{\Gamma \tau / [\Gamma \tau + (e^{2r} - 1)(1 - e^{-\Gamma \tau})]}$  [25]. One thus only needs a modest bandwidth, e.g.  $\Gamma \sim 10\kappa$  is enough for  $\kappa \tau \sim 10$  and  $e^{2r} \sim 10$ .

The lack of any enhanced Purcell decay is also crucial, as in our protocol the squeezing is turned on well before the coherent measurement tone. Having a finite squeezing bandwidth can in fact be an advantage as it helps suppress Purcell decay of the qubit. This decay corresponds to relaxation of the qubit by photon emission from the cavity [30]. As typical detunings  $\Delta \gg \kappa$ , there is a wide range of ideal squeezing bandwidths satisfying  $\kappa \ll \Gamma \ll \Delta$ . Such bandwidths are large enough to allow a full enhancement of the SNR (with  $\tau \gtrsim 1/\kappa$ ), and small enough that the squeezing does not appreciably modify cavity-induced Purcell decay (see [25]).

Another non-ideality is asymmetry in the system parameters. While the two cavity frequencies can differ, we have assumed so far that they have identical damping rates ( $\kappa_1 = \kappa_2 = \kappa$ ) and that the dispersive coupling strengths satisfy  $\chi_1 = -\chi_2 = \chi$ . Deviation from either of these conditions breaks the symmetry yielding a QMFS, causing an unwanted coupling between the squeezed quadratures ( $\hat{X}_-, \hat{Y}_+$ ) and the anti-squeezed quadratures ( $\hat{X}_+, \hat{Y}_-$ ). The structure of the QMFS can persist in the presence of asymmetries for long measurement times  $\kappa \tau \gg 1$ , under the condition [25]

$$\frac{\chi_1 + \chi_2}{\chi_1 - \chi_2} = \frac{\kappa_1 - \kappa_2}{\kappa_1 + \kappa_2}. \quad (4)$$

The SNR enhancement can however be preserved for measurement times  $\tau \sim 1/\kappa$  by optimizing  $\delta\kappa/\delta\chi$ , as illustrated in Fig. 4(a). Although this might not be necessary in practice, all parameters in Eq. (4) can be tuned in situ [18, 31, 32] thereby greatly relaxing the constraints

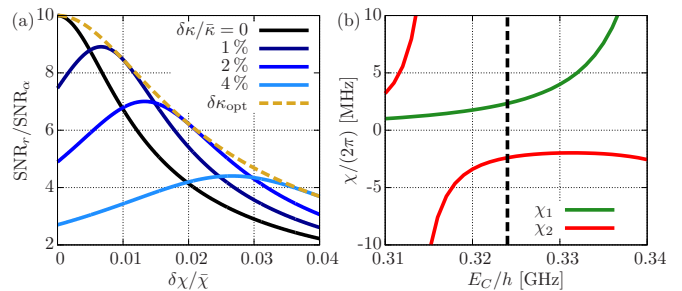


FIG. 4. (a) SNR enhancement as a function of the dispersive shift asymmetry ( $\chi_{1,2} = \delta\chi \pm \bar{\chi}$ ) for different resonator linewidth asymmetries ( $\kappa_{1,2} = \bar{\kappa} \pm \delta\kappa$ ) calculated for  $\bar{\chi} = \bar{\kappa}/2$ ,  $\kappa\tau = 10$  and  $e^{2r} = 100$ . The dashed line is the maximal SNR obtained by optimizing  $\delta\kappa$ . (b) Calculated dispersive shifts as a function of transmon anharmonicity  $E_C$  from a numerical diagonalization of transmon-resonator system for each of the resonators. The parameters are  $E_J/h = 25$  GHz,  $\omega_1/2\pi = 7.6$  GHz,  $\omega_2/2\pi = 7.9$  GHz,  $g_1/2\pi = 8$  MHz and  $g_2/2\pi = 15$  MHz. The vertical dashed line shows a typical value of  $E_C$  that leads to equal and opposite dispersive shifts.

on the system.

Finally, like any scheme employing squeezing, photon losses effectively replace squeezed fluctuations with ordinary vacuum, causing the SNR improvement to saturate as a function of squeezing strength [25]. Despite this, our scheme still yields considerable advantages for finite loss rates, see Figs. 3(b) and (c).

*Implementation in circuit QED*— We now turn to a possible realization of this protocol in circuit QED. All parameters discussed here are readily achievable experimentally. As illustrated in Fig. 2, a transmon qubit is coupled to two resonators, one in the usual dispersive regime ( $\Delta > E_C$ ) while the other in the ‘straddling’ regime ( $\Delta < E_C$ ) [18, 33]. Here,  $\Delta$  is the qubit-resonators detuning and  $E_C$  the transmon anharmonicity. This yields dispersive couplings  $\chi$  having opposite signs as required, see Fig. 4(b). An alternative strategy is to use a fluxonium or a flux qubit which exhibit a richer dispersive shift profile [34]. Note that either approach does not entail a sacrifice of qubit coherence via enhanced Purcell decay [25]. The displaced two-mode squeezed state required at the input can either be generated by a NDPA such as the Josephson parametric converter [27], a Josephson paramp [35] or the Bose-Hubbard dimer [28].

*Conclusion*— We have presented a realistic measurement protocol that allows one to exponentially enhance dispersive measurement using two-mode squeezed light, enabling Heisenberg-limited scaling even with large dispersive couplings. Our scheme crucially makes use of a special symmetry in the dynamics of joint cavity quadratures, a so-called “quantum-mechanics-free subsystem”.

*Acknowledgements*— We thank Irfan Siddiqi, Michel Devoret, Shabir Barzanjeh, Samuel Boutin, Shruti Puri, Baptiste Royer and Amit Munje for many useful dis-

cussions. This work was supported by the Army Research Office under Grant W911NF-14-1-0078, INTRIQ, NSERC and CIFAR.

- 
- [1] V. Giovannetti, S. Lloyd, and L. Maccone, *Science* **306**, 1330 (2004).
- [2] C. Caves, *Phys. Rev. D* **23**, 1693 (1981).
- [3] B. Yurke, S. McCall, and J. Klauder, *Phys. Rev. A* **33**, 4033 (1986).
- [4] V. B. Braginsky, Y. I. Vorontsov, and K. S. Thorne, *Science* **209**, 547 (1980).
- [5] C. Caves, K. Thorne, R. Drever, V. Sandberg, and M. Zimmermann, *Rev. Mod. Phys.* **52**, 341 (1980).
- [6] V. B. Braginsky, F. Y. Khalili, and K. S. Thorne, *Quantum Measurement* (Cambridge University Press, 1995).
- [7] The LIGO Scientific Collaboration, *Nat. Phys.* **7**, 962 (2011).
- [8] The LIGO Scientific Collaboration, *Nat. Photon.* **7**, 613 (2013).
- [9] K. Iwasawa, K. Makino, H. Yonezawa, M. Tsang, A. Davidovic, E. Huntington, and A. Furusawa, *Phys. Rev. Lett.* **111**, 163602 (2013).
- [10] M. A. Taylor, J. Janousek, V. Daria, J. Knittel, B. Hage, B. Hans-A., and W. P. Bowen, *Nat. Photon.* **7**, 229 (2013).
- [11] M. A. Nielsen and I. L. Chuang, *Quantum Computation and Quantum Information* (Cambridge University Press, 2000).
- [12] A. Blais, R.-S. Huang, A. Wallraff, S. Girvin, and R. Schoelkopf, *Phys. Rev. A* **69**, 062320 (2004).
- [13] E. Jeffrey, D. Sank, J. Y. Mutus, T. C. White, J. Kelly, R. Barends, Y. Chen, Z. Chen, B. Chiaro, A. Dunsworth, A. Megrant, P. J. J. O'Malley, C. Neill, P. Roushan, A. Vainsencher, J. Wenner, A. N. Cleland, and J. M. Martinis, *Phys. Rev. Lett.* **112**, 190504 (2014).
- [14] Y. Liu, S. J. Srinivasan, D. Hover, S. Zhu, R. McDermott, and A. A. Houck, *New J. Phys.* **16**, 113008 (2014).
- [15] Z. R. Lin, K. Inomata, W. D. Oliver, K. Koshino, Y. Nakamura, J. S. Tsai, and T. Yamamoto, *Appl. Phys. Lett.* **103**, 132602 (2013).
- [16] S. Barzanjeh, D. P. DiVincenzo, and B. M. Terhal, *Phys. Rev. B* **90**, 134515 (2014).
- [17] M. Tsang and C. Caves, *Phys. Rev. X* **2**, 031016 (2012).
- [18] J. Koch, T. Yu, J. Gambetta, A. Houck, D. Schuster, J. Majer, A. Blais, M. Devoret, S. Girvin, and R. Schoelkopf, *Phys. Rev. A* **76**, 042319 (2007).
- [19] M. Tsang and C. Caves, *Phys. Rev. Lett.* **105**, 123601 (2010).
- [20] W. Wasilewski, K. Jensen, H. Krauter, J. Renema, M. Balabas, and E. Polzik, *Phys. Rev. Lett.* **104**, 133601 (2010).
- [21] M. Woolley and A. Clerk, *Phys. Rev. A* **87**, 063846 (2013).
- [22] K. Zhang, P. Meystre, and W. Zhang, *Phys. Rev. A* **88**, 043632 (2013).
- [23] J. Gambetta, A. Blais, M. Boissonneault, A. A. Houck, D. I. Schuster, and S. M. Girvin, *Phys. Rev. A* **77**, 012112 (2008).
- [24] A. Clerk, M. Devoret, S. Girvin, F. Marquardt, and R. Schoelkopf, *Rev. Mod. Phys.* **82**, 1155 (2010).
- [25] See Supplemental Material, which includes Refs. [36, 37].
- [26] P. D. Drummond and Z. Ficek, eds., *Quantum Squeezing* (Springer, 2004).
- [27] E. Flurin, N. Roch, F. Mallet, M. Devoret, and B. Huard, *Phys. Rev. Lett.* **109**, 183901 (2012).
- [28] C. Eichler, Y. Salathe, J. Mlynek, S. Schmidt, and A. Wallraff, *Phys. Rev. Lett.* **113**, 110502 (2014).
- [29] D. Walls and G. J. Milburn, *Quantum Optics*, 2nd ed. (Springer, 2008).
- [30] A. A. Houck, J. A. Schreier, B. R. Johnson, J. M. Chow, J. Koch, J. M. Gambetta, D. I. Schuster, L. Frunzio, M. H. Devoret, S. M. Girvin, and R. J. Schoelkopf, *Phys. Rev. Lett.* **101**, 080502 (2008).
- [31] M. Sandberg, C. M. Wilson, F. Persson, T. Bauch, G. Johansson, V. Shumeiko, T. Duty, and P. Delsing, *Appl. Phys. Lett.* **92**, 203501 (2008).
- [32] Y. Yin, Y. Chen, D. Sank, P. J. J. O'Malley, T. C. White, R. Barends, J. Kelly, E. Lucero, M. Mariantoni, A. Megrant, C. Neill, A. Vainsencher, J. Wenner, A. N. Korotkov, A. N. Cleland, and J. M. Martinis, *Phys. Rev. Lett.* **110**, 107001 (2013).
- [33] K. Inomata, T. Yamamoto, P.-M. Billangeon, Y. Nakamura, and J. Tsai, *Phys. Rev. B* **86**, 140508 (2012).
- [34] G. Zhu, D. Ferguson, V. Manucharyan, and J. Koch, *Phys. Rev. B* **87**, 024510 (2013).
- [35] C. Eichler, D. Bozyigit, C. Lang, M. Baur, L. Steffen, J. Fink, S. Filipp, and A. Wallraff, *Phys. Rev. Lett.* **107**, 113601 (2011).
- [36] C. Gardiner and P. Zoller, *Quantum Noise*, 3rd ed. (Springer, 2004).
- [37] M. Boissonneault, J. Gambetta, and A. Blais, *Phys. Rev. A* **79**, 013819 (2009).